Available online at www.sciencedirect.com
SCIENCE DIRECT®
Optics Communications 219 (2003) 277–283
OPTICS COMMUNICATIONS
www.elsevier.com/locate/optcom

Subcollinear acousto-optic tunable filter based on the medium with a strong acoustic anisotropy

Alexei K. Zaitsev[a,*], Viktor V. Kludzin[b]

[a] *Institute of Electro-Optical Engineering, National Chiao Tung University, 1001 TaHsueh Rd., Hsinchu 30050, Taiwan*
[b] *St. Petersburg State University of Aerospace Instrumentation, 67 Bolshaya Morskaya St., St. Petersburg 190000, Russia*

Received 1 May 2002; received in revised form 4 December 2002; accepted 2 February 2003

Abstract

We design and investigate the properties of acousto-optical tunable filter (AOTF) based on tellurium dioxide (TeO_2) single crystal. We use so-called "subcollinear" geometry of anisotropic acousto-optic interaction that occurs when the wavevector of incident light is collinear to acoustic energy vector. We have obtained the analytical formula of spectrum spread function of proposed AOTF and have found the condition determining the shape of that characteristic. Also we have designed and fabricated the experimental prototype of subcollinear AOTF. In our design we have used the reflection of acoustic wave that allowed to use crystal's media more effectively and reduce the AOTF size. The main advantage of filter based on proposed geometry is extremely low value of electrical driving power (20 mW) that makes it a strong candidate in many applications.

PACS: 42.79.Jq; 78.20.Hp

Keywords: Acousto-optic tunable filter; Anisotropy; Tellurium dioxide

1. Introduction

In recent years the results on research of acousto-optic tunable filters (AOTF) operating in ultraviolet, visible and infrared regions of spectrum have achieved a great progress. High spectral and spatial resolution, perfect diffraction efficiency and low driving power provide application of the filters in optics and spectroscopy as well as in optical information processing, telecommunication and laser technology [1–3]. Precise and efficient electronic control of laser light intensity and fast electronic tuning of lasing wavelength can be executed by means of acousto-optic devices. Application of AOTFs as selectors of arbitrary polarized optical signals in modern WDM communication lines has also demonstrated high capabilities of the acousto-optic instruments.

One of problems of high-resolution acousto-optic tunable filters (AOTF) is to make an acousto-optic cell with a large length of interaction.

* Corresponding author. Tel.: +886-3-571-2121x56329; fax: +886-3-571-6631.
E-mail address: akz@cc.nctu.edu.tw (A.K. Zaitsev).

0030-4018/03/$ - see front matter © 2003 Elsevier Science B.V. All rights reserved.
doi:10.1016/S0030-4018(03)01293-8

The traditionally used cells based on an orthogonal diffraction have a disadvantage that their interaction length is determined by the size of the piezoelectric transducer [4]. In addition, a large transducer has a high capacitance and small electrical resistance, which is extremely inconvenient. Therefore, in this case, segmented transducers are usually used. However, such partitioning procedure results in more complex AOTF construction and more complex matching of a piezoelectric transducer with an RF signal generator.

For this reason, the collinear AOTFs are more practical as their lengths of interaction do not depend on the transducer's size and their lengths are determined potentially only by available crystal length. The collinear geometry of acousto-optical interaction has many advantages, but it exists in a limited number of crystals: α-SiO_2, $LiNbO_3$, $CaWO_4$, $CaMoO_4$ [4].

The single crystal of tellurium dioxide (TeO_2) has a rather high acousto-optic figure of merit [5]. But strict collinear diffraction is impossible in this material. At deviations from crystal axis, there is a considerable mismatch between acoustic energy direction (or group velocity) and acoustic wave vector due to high ultrasonic anisotropy in TeO_2 [6].

The last feature makes the subcollinear diffraction possible, which is also called as "collinear beam" and represents a case of an anisotropic diffraction when the wave vector of an incident light is collinear to acoustic energy vector. Such geometry of interaction was proposed for the first time in α-quartz [7]. Later [8–11] that kind of geometry was realized in paratellurite which has much stronger acoustic anisotropy. It is obvious, that for subcollinear geometry the length of interaction does not depend on the size of piezoelectric transducer, which is similar to the collinear diffraction. That important feature was already mentioned in recent references [8–11].

In this paper we investigate the main characteristics of subcollinear AOTF, its spectrum spread function, which is very different from both conventional orthogonal and collinear type of acousto-optic interaction. We also design the AOTF prototype's layout which uses the reflection of acoustic wave instead of optic one [9].

2. Acousto-optic interaction in the media with a strong acoustic anisotropy

It is known that strict collinear diffraction is impossible in the TeO_2 crystal. However, high-resolution acousto-optic tunable filters can be made of this crystal due to the combination of its unique properties (high acousto-optic quality, low velocity of slow shear mode, strong acoustic anisotropy). An interesting variant of anisotropic diffraction in this material was suggested by Voloshinov [8,9].

In this diffraction geometry (Fig. 1), the acoustic vector of wave normal $\mathbf{K}_a$ is oriented with an angular deviation from the [1 1 0]-axis in the $(1\ \bar{1}\ 0)$-plane. Due to the elastic anisotropy which is quite essential for this crystal, there is a considerable angle mismatch Ψ between the direction of the wave normal and energy transport $\mathbf{v}_g$ [6,12].

$$\psi = \operatorname{arctg}\left(\frac{1}{2}\frac{\sin 2\Theta_a\left(\frac{C_{11}-C_{12}}{2}-C_{44}\right)}{\frac{C_{11}-C_{12}}{2}\sin^2\Theta_a + C_{44}\cos^2\Theta_a}\right), \qquad (1)$$

where C_{mn} denote the elastic constants of TeO_2 and Θ_a is the angle between [0 0 1]-axis and the acoustic vector of wave normal $\mathbf{K}_a$. The angles Θ_i and Θ_d determine the direction of incident and diffracted light vector relative to [0 0 1]-axis, respectively. It should be mentioned that introduced coordinates (x, y, z) do not coincide with the main crystal axes. Namely, the y-axis coincides with the $[1\ \bar{1}\ 0]$ crystal

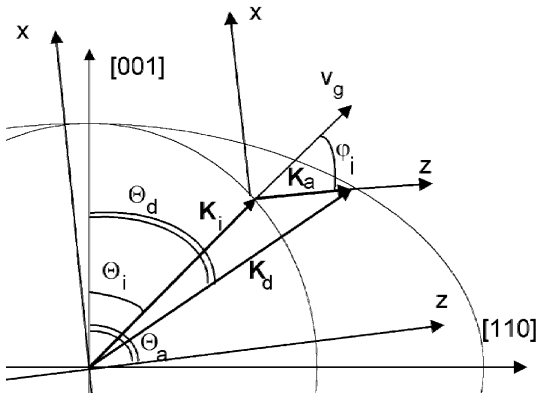

Fig. 1. Wave vector diagram for the subcollinear diffraction in TeO_2.

axis, and the plane (x,z) is rotated by the angle Θ_a with respect to the (1 1 0)-plane so that z-direction coincides with the acoustic vector of wave normal $\mathbf{K}_a$ (see Fig. 1).

As the incident light vector $\mathbf{K}_i$ is directed along the direction of acoustic energy transfer, such geometry may be called as "collinear by the group velocities", "beam collinear" or "subcollinear".

Let us analyze the acoustic wave generated by a flat piezoelectric transducer with dimensions $D \times h$ and propagated in the finite dimension L.

Without mentioned limitations, a plane acoustic wave travelling in z-direction may be treated as

$$\begin{aligned} A(t,z) &= A_0 \exp[\mathrm{j}(\Omega_0 t + K_{zo} z)] \\ &= A_0 \exp\left[\mathrm{j}\left(2\pi f_0 t + \frac{2\pi f_0}{v_0} z\right)\right], \end{aligned} \tag{2}$$

where v_0 is the acoustic wave velocity in the z-direction, f_0 is the central frequency supplied to the transducer.

Let us assume that the limitation in the propagation dimension L allows us to represent the acoustic field as a spectrum of spatial frequencies $S(K)$ (or wave numbers) and to use the spatial Fourier transform to calculate it. We can write

$$\begin{aligned} \dot{S}(K) &= \int_{-\infty}^{\infty} A(z, t=0) \exp(-\mathrm{j} K_z z)\,\mathrm{d}z \\ &= \int_{-L/2}^{L/2} A_0 \exp[\mathrm{j}(K_{z0} - K_z) z]\,\mathrm{d}z \\ &= A_0 L \mathrm{sinc}\left[(K_{zo} - K_z)\frac{L}{2}\right], \end{aligned} \tag{3}$$

that physically shows the amplitude E_k of a partial wave with the wave number K_z travelling in the z-direction.

$$\begin{aligned} e_a(t,z,K_z) &= A_0 L \mathrm{sinc}\left[(K_{zo} - K_z)\frac{L}{2}\right] \exp[\mathrm{j}(\Omega_0 t + K_z z)] \\ &= E_k \exp[\mathrm{j}(\Omega_0 t + K_z z)], \end{aligned} \tag{4}$$

where wave number $K_z = 2\pi f / v_0$.

Moreover, the transducer's finite dimension D results in the limitation in spatial aperture of each wave that also allows to represent the acoustic field in the components of angular spectrum [13]

$$\begin{aligned} \dot{A}(\varphi) &= \int_{-\infty}^{\infty} E_k \exp(-\mathrm{j} K_x x)\,\mathrm{d}x \\ &= \int_{-D/2}^{D/2} E_k \exp\left(-\mathrm{j}\frac{2\pi f}{v(\varphi)} x\right)\mathrm{d}x \\ &= \frac{E_k D}{2} \mathrm{sinc}\left(\frac{2\pi f}{v(\varphi)} \sin(\varphi)\frac{D}{2}\right). \end{aligned} \tag{5}$$

At that, each partial component of the angular spectrum travels with its own velocity $v(\varphi)$ and angle φ to the z-axis.

As a result, the acoustic field in the medium of interaction can be represented as a superposition of the waves in the following form

$$\begin{aligned} e_a(t,x,z,\varphi,f) =& \dot{A}(\varphi, f) \exp[\mathrm{j}(\Omega_0 t + K_{\varphi z} z + K_{\varphi x} x)] \\ =& \frac{A_0 L D}{2} \mathrm{sinc}\left(\frac{2\pi(f - f_0)}{v_0}\frac{L}{2}\right) \\ & \times \mathrm{sinc}\left(\frac{2\pi f}{v(\varphi)} \sin(\varphi)\frac{D}{2}\right) \\ & \times \exp\left[\mathrm{j}\left(\Omega_0 t + \frac{2\pi f}{v(\varphi)} \cos(\varphi) z \right.\right. \\ & \left.\left. + \frac{2\pi f}{v(\varphi)} \cos(\varphi) z + \frac{2\pi f}{v(\varphi)} \sin(\varphi) x\right)\right]. \end{aligned} \tag{6}$$

Let the following plane optical wave come into the acousto-optic cell,

$$\begin{aligned} e_i(t,x,z) &= E_i \exp[\mathrm{j}(\omega t + k_x x + k_z z)] \\ &= E_i \exp\left[\mathrm{j}\left(\omega t + \frac{2\pi n_i}{\lambda} \sin\varphi_i x \right.\right. \\ &\quad \left.\left. + \frac{2\pi n_i}{\lambda} \cos\varphi_i z\right)\right], \end{aligned} \tag{7}$$

where λ is the wavelength, ω is the optical frequency, n_i is the refractive index of media corresponding to propagating wave and φ_i is the angle between the wave normal of the incident light and the z-axis. Let the Bragg synchronism condition for the anisotropic diffraction is correct for the main component ($\varphi = 0$, $f = f_a$) of the plane acoustic wave superposition (6). At that, the synchronism condition looks like [10]

$$\frac{\lambda f_a}{v_0 \Delta n} = \frac{\sin^2 \Theta_i}{\cos(\Theta_i - \Theta_a)}, \tag{8}$$

where Δn is crystal's birefringence, f_a is a Bragg synchronism frequency, Θ_i and Θ_a are the angles determining the wave normals of the optical and acoustical vectors with respect to the [0 0 1]-axis in the $(1\,\bar{1}\,0)$-plane.

In the designations of Fig. 1, the synchronism condition can be rewritten as

$$\frac{\lambda f_a}{v_0 \Delta n} = \frac{\sin^2(\Theta_a - \varphi_i)}{\cos\varphi_i}. \tag{9}$$

Because of acoustic anisotropy, the diffraction of the same optical wave is possible not only on the main but also on the other spectrum components of acoustic field (6). This occurs when the following condition is fulfilled

$$\frac{\lambda f}{v(\varphi)\Delta n} = \frac{\sin^2(\Theta_a - \varphi_i)}{\cos(\varphi_i + \varphi)}. \tag{10}$$

where $v(\varphi)$ is the dependence of acoustic wave velocity on the propagation direction, which can be assumed in the $(1\,\bar{1}\,0)$-plane as [6]

$$v(\varphi) = \sqrt{\frac{\frac{C_{11}-C_{12}}{2}\sin^2(\Theta_a + \varphi) + C_{44}\cos^2(\Theta_a + \varphi)}{\rho}}, \tag{11}$$

where ρ is the medium's density.

In order to calculate the diffracted light field, it is necessary to determine all spectral components that are diffracting and summarize the diffraction results from those components. Obviously, this technique uses the superposition principle and is correct for the weak acousto-optic interaction only.

Strictly speaking, the acousto-optic figure of merit M_2 is different for different spectral components of the acoustic field. But practically the range of φ is small and thus M_2 changes not much and can be assumed as a constant.

Generally, there are infinite number of the diffracting plane waves which parameters (f, φ) form combinations satisfied the synchronism condition (10). Therefore, one parameter can be expressed from the other by using the above mentioned equations

$$f = \frac{f_a v(\varphi)\cos\varphi_i}{v_0\cos(\varphi_i + \varphi)} = f(\varphi). \tag{12}$$

The expression for the diffracted light field as a superposition of plane optical waves can be written

$$e_d(t,x,z) = \frac{1}{2\pi}\int_{-\pi/2}^{\pi/2} e_i(t,x,z)e_a(t,x,z,\varphi,f(\varphi))\,d\varphi. \tag{13}$$

We are interested about the intensity of the diffracted field that can be calculated in the following way

$$I_d = \lim_{C\to\infty}\frac{1}{C}\int_{-C/2}^{C/2} e_d(t,x,z_0)e_d^*(t,x,z_0)\,dx. \tag{14}$$

Substituting (6), (7), (12) and (13) into (14), we can obtain the formula for diffracted intensity

$$I_d(f_0) = C_1\int_{-\pi/2}^{\pi/2}\mathrm{sinc}^2\left(\frac{\pi L}{v_0}\left(\frac{f_a v(\varphi)\cos\varphi_i}{v_0\cos(\varphi_i+\varphi)} - f_0\right)\right) \times \mathrm{sinc}^2\left(\frac{2\pi f_a}{v_0}\frac{\cos\varphi_i\sin\varphi}{\cos(\varphi_i+\varphi)}\frac{D}{2}\right)d\varphi. \tag{15}$$

It should be noted that when the other parameters are constant the dependance of I_d on f_0 means the frequency response to a monochromatic (laser) input signal or the spectrum spread function of the device.

In order to analyze (15), we represent the expression for the acoustic wave velocity (11) under a small deviation of the angle φ in the following form [12]

$$v(\varphi) = v_o(1 + a\varphi + b\varphi^2), \tag{16}$$

where a characterizes the "walk-off" angle and b is the acoustic field spread.

Then we substitute (16) into (12), expand the expression (12) for the frequency into a power series and confine it to three members

$$f(\varphi) = f_a\left[1 + (a + tg\varphi_i)\varphi + \left(b + \frac{1}{2} + tg\varphi_i(a + tg\varphi_i)\right)\varphi^2\right]. \tag{17}$$

In our case the subcollinearity condition $a = -\tan\varphi$ is correct. Then the frequency of synchronism changes on the angle according to the parabolic law

$$f(\varphi) = f_a\left[1 + \left(b + \frac{1}{2}\right)\varphi^2\right]. \tag{18}$$

Let us substitute (18) into (15) and analyze the integral. There is a product of two functions in it. When the second sinc^2 is much narrower than the first one, that is when

$$\sqrt{\frac{v_0 L(b+0.5)}{f_a D^2}} \ll 1, \tag{19}$$

the filter's spectral response does not depend on the acoustic field spread and is determined by the interaction length L only and has the form

$$I_d(f_0) = C_2 \mathrm{sinc}^2\left(\frac{\pi L}{v_0}(f_a - f_0)\right). \tag{20}$$

When Condition (19) is not fulfilled, the filter's spectral response considerably depends on the transducer's dimensions and anisotropic properties of the medium. According to (15), a dependence of the diffraction intensity on the frequency mismatch for an acousto-optic tunable filter based on the subcollinear interaction geometry is calculated (Fig. 2). The filter's parameters are: the incident angle Θ_i is 30°, the angle Θ_a is 80°, the interaction length L is 42 mm, the transducer dimension D is 2 mm, the frequency of Bragg synchronism f_a is 66.2 MHz, and the wavelength λ is 633 nm.

It is interesting that the shape of the spectral response is clearly unsymmetrical.

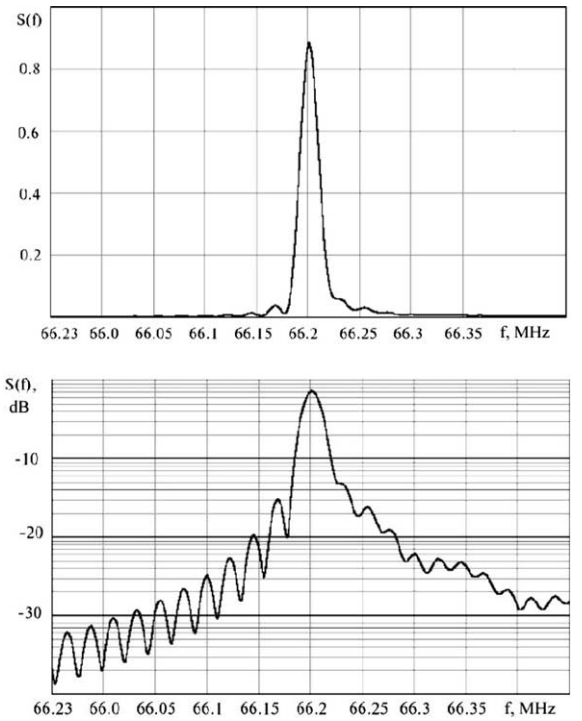

Fig. 2. Filter's calculated spectrum spread function in linear and logarithmic scales.

3. AOTF design and experimental measurements

The advantage of proposed interaction geometry is the fact that for this geometry (similar to the collinear diffraction) the transducer dimension does not determine the interaction length that can be rather long (practically up to 50 mm).

According to theoretical calculation of previous chapter, an experimental prototype of acousto-optic tunable filter have been made. For the maximum M_2, the incident angle was chosen $\Theta_i = 30°$ [10].

For practical manufacturing, it is clear that the reflection of either optical or acoustic wave from the optical face has to be used in order to generate the acoustic wave with the required orientation, otherwise transducer could shade the interaction medium from the incident light.

In order to minimize the cell's size we have chosen the variant of acoustic reflection (Fig. 3). The piezoelectric transducer irradiates shear acoustic wave with wave normal $\mathbf{K}_{a1}$, which shifting vector is parallel to the surface of reflecting facet. The vector $\mathbf{v}_{g1}$ shows the direction of energy transport of irradiated wave. The acoustic reflection happens without of wave polarization transformation and is characterized by high energy transfer coefficient. The reflected acoustic wave has the wave normal $\mathbf{K}_{a2}$ and the energy transport $\mathbf{v}_{g2}$. It should be mentioned that due to strong acoustic

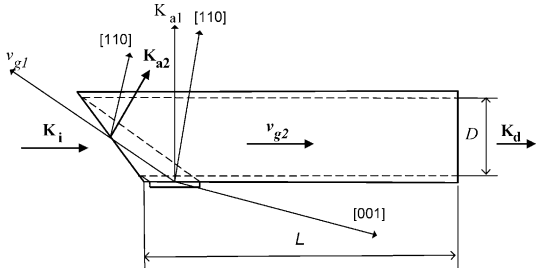

Fig. 3. The prototype's layout.

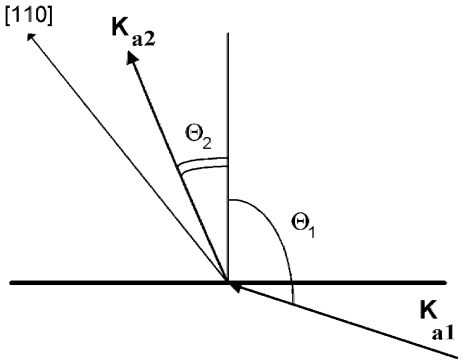

Fig. 4. The geometry of acoustic reflection on the facet.

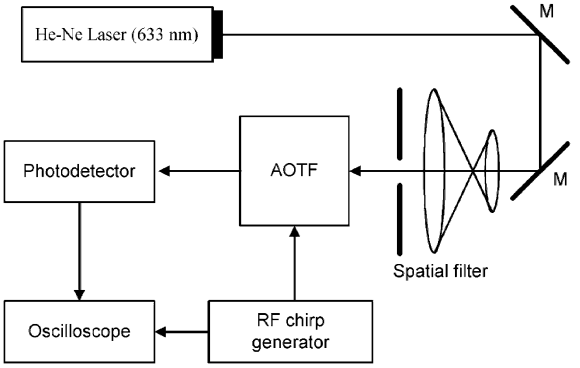

Fig. 5. Experimental setup for AOTF response measurement.

anisotropy of TeO_2, the reflection on the facet occurs when the incident angle is larger than 90°. The geometry of acoustic reflection is shown in Fig. 4. The Snell's law is still correct in this case and we can write

$$\frac{\sin \Theta_1}{v_1} = \frac{\sin \Theta_2}{v_2}, \tag{21}$$

where Θ_1, Θ_2 and v_1, v_2 are angles and velocities of incident and reflected acoustic waves, respectively.

An incident optical wave corresponding to ordinary polarization is diffracted on reflected acoustic wave. The vector of wave normal of optical wave $\mathbf{K}_i$ is coincided with the energy transport of acoustic wave $\mathbf{v}_{g2}$. The diffracted optical wave with wave normal $\mathbf{K}_d$ corresponds to extraordinary polarization (Fig. 3).

It is important that designed prototype is very compact. The volume of crystal is used almost completely. This is the advantage of our design under the previous one that used an optical reflection [9].

To prove the theoretical prediction we have measured the frequency response of fabricated AOTF. The experimental setup for the measurement is shown in Fig. 5. After beam expansion we apply a monochromatic linear polarized light of He–Ne laser with wavelength $\lambda = 633$ nm to the input of our AOTF prototype. The radio frequency generator which frequency varies from 65.95 to 66.45 MHz was connected to the transducer of AOTF. The photodetector measures the intensity of diffracted light beam and gives the information about relative diffraction efficiency. The oscilloscope shows its value in dependence of the frequency of control signal.

Table 1
The parameters of subcollinear AOTF prototype

Incident angle, Θ_i	30°
Angle, Θ_a	80°
Interaction length, L	42 mm
Optical aperture, D	2 mm
Diffraction angle, Θ_d	1.2°
Acoustic power for 80% efficiency ($\lambda = 633$ nm)	20 mW
Spectral resolution, $\delta\lambda$ ($\lambda = 633$ nm)	0.3 nm
Angular aperture, $\delta\Theta$	0.04°
AO cell dimensions	$7 \times 7 \times 42$ mm

Table 1 shows the parameters of the experimental AOTF prototype and Fig. 6 shows its experimental frequency response in the linear and logarithmic scales.

4. Discussion

The experimental results show that when a uniformly collimated light beam comes onto the cell, the spectral characteristic of transmission has a strongly asymmetrical shape. It can be explained by the fact that the finite size of piezoelectric transducer results in plane waves generated in an anisotropic medium of interaction. The velocity of plane waves varies unevenly at a deviation from the main component. The diffraction on these components results in an asymmetrical shape of spectral response. That matches well the theory.

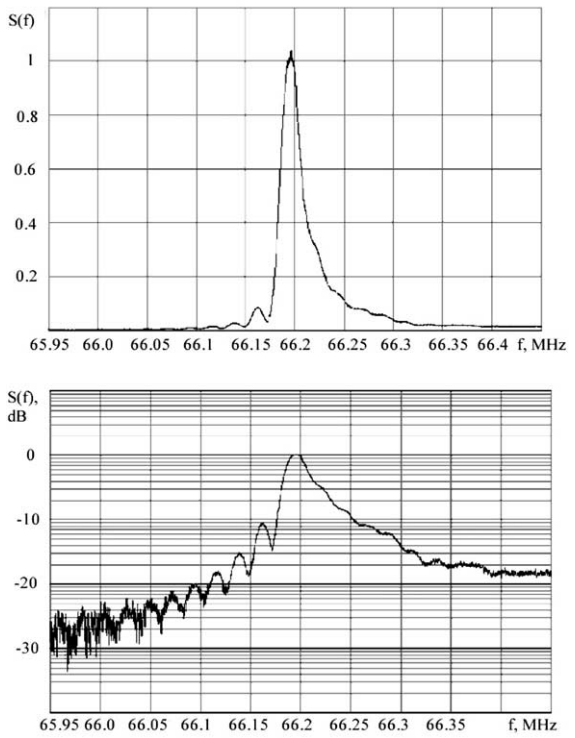

Fig. 6. Filter's experimental response in linear and logarithmic scales.

It is important to note some features of fabricated subcollinear filter:

(1) It requires extremely low drive power to obtain a high diffraction efficiency (20 mW for 80%). This is due to the long length of interaction and high value of M_2.

(2) It has a high spectral resolution (0.3 nm at 633 nm central wavelength).

(3) It has a very small angular aperture (0.04°) and is very sensitive to the collimation quality and beam uniformity of incident light. In practice, the frequency response could be obtained only when the filter was illuminated by a wide collimated beam. In the case of Gaussian beam using, the spectral resolution decreases and the shape of characteristic loses asymmetry and becomes also Gaussian.

5. Conclusion

We design and investigate the properties of subcollinear AOTF based on the media with a strong acoustic anisotropy, tellurium dioxide single crystal. The advantage of proposed AOTF is that the length of interaction in this case does not dependent on the transducer size and could be chosen a significant value. We have obtained the analytical formula of spectrum spread function of proposed AOTF and have found the condition determining the shape of that characteristic. We also fabricated the experimental prototype of subcollinear AOTF. At designing of AOTF prototype we have used the reflection of acoustic wave that allows to minimize the dimensions of AO cell. Our experimental results of fabricated AOTF prove the theoretical predictions.

The spectral response of an AOTF being in an anisotropic mode of interaction in an ultrasonically anisotropic medium has asymmetrical shape. That sufficient asymmetry is exhibited in a case when: (1) the angle between a wave normal of an incident light and a vector of ultrasonic energy transport is small (subcollinearity condition); (2) interactions are carried out up to a far-field region of a piezoelectric transducer, that mathematically means not realization of a requirement (19).

References

[1] T. Chikama, H. Onaka, S. Kuroyanagi, Fujitsu Sci. Technical J. 35 (1999) 46.
[2] C.D. Tran, Talanta 45 (1997) 237.
[3] V.B. Voloshinov, V.N. Parygin, V.Y. Molchanov, Proc. SPIE 4353 (2001) 17.
[4] A.P. Goutzolis, D.R. Pape (Eds.), Design and Fabrication of Acousto-Optic Devices, Markel Dekker, New York, 1994, p. 497.
[5] N. Uchida, Y. Ohmachi, J. Appl. Phys. 40 (1969) 4692.
[6] Y. Ohmachi, N. Uchida, N. Niizeki, JASA (1972) 164.
[7] J.A. Kusters, D.A. Wilson, D.L. Hammond, JOSA 64 (1974) 434.
[8] V.B. Voloshinov, Opt. Eng. 31 (1992) 2089.
[9] V.B. Voloshinov, V.Y. Molchanov, V.N. Parygin, V.S. Toupitza, Sov. Technical Phys. Lett. 18 (1992) 33.
[10] I.C. Chang, Electron. Lett. 28 (1992) 1255.
[11] C.S. Qin, G.C. Huang, K.T. Chan, K.W. Cheung, Electron. Lett. 31 (1995) 1237.
[12] R. Truell, C. Elbaum, B. Chick, in: Ultrasonic Methods in Solid State Physics, Academic Press, London, UK, 1969, p. 464.
[13] J.W. Goodman, in: Introduction to Fourier Optics, McGraw Hill, New York, 1968, p. 287.